Hindawi
Complexity
Volume 2022, Article ID 2174806, 14 pages
https://doi.org/10.1155/2022/2174806

Research Article

Soliton Solutions of Generalized Third Order Time-Fractional KdV Models Using Extended He-Laplace Algorithm

Mubashir Qayyum,[1] **Efaza Ahmad**,[1] **Sidra Afzal**,[1] **and Saraswati Acharya**[2]

[1]*Department of Sciences and Humanities, National University of Computer and Emerging Sciences, Lahore, Pakistan*
[2]*Kathmandu University School of Science, Dhulikhel, Nepal*

Correspondence should be addressed to Saraswati Acharya; saraswati.acharya@ku.edu.np

Received 29 August 2022; Accepted 8 October 2022; Published 25 October 2022

Academic Editor: Abdellatif Ben Makhlouf

Copyright © 2022 Mubashir Qayyum et al. This is an open access article distributed under the Creative Commons Attribution License, which permits unrestricted use, distribution, and reproduction in any medium, provided the original work is properly cited.

In this research, the He-Laplace algorithm is extended to generalized third order, time-fractional, Korteweg-de Vries (KdV) models. In this algorithm, the Laplace transform is hybrid with homotopy perturbation and extended to highly nonlinear fractional KdVs, including potential and Burgers KdV models. Time-fractional derivatives are taken in Caputo sense throughout the manuscript. Convergence and error estimation are confirmed theoretically as well as numerically for the current model. Numerical convergence and error analysis is also performed by computing residual errors in the entire fractional domain. Graphical illustrations show the effect of fractional parameter on the solution as 2D and 3D plots. Analysis reveals that the He-Laplace algorithm is an efficient approach for time-fractional models and can be used for other families of equations.

1. Introduction

In the last few decades, fractional calculus has outperformed ordinary calculus because basic calculus has reached to its peak. Engineers and scientists are focusing on the fractional models and their solutions due to their ability to provide more meaningful insight of physical phenomena with memory effects such as fractional Casson fluid with ramped wall temperature [1], fractional SEIR model of Covid 19 [2], fractional dual-phase-lag thermoelastic model [3], novel fractional time-delayed grey Bernoulli forecasting model [4], fractal fractional model of drilling nono-liquids [5] and stability of fractional quasi-linear impulsive integro-differential systems [6]. This permits a more accurate description of real-world situations than the basic integral order. Well-known scientists including Joseph [7], Miller and Ross [8], Caputo [9], and Riemann [10] have made a significant contribution towards the foundation of fractional calculus. Fractional calculus provides a more accurate and realistic depiction of various phenomena in quantum physics [11], oceanography [12], fluid mechanics [13], and engineering [14]. In addition, fractional calculus is used to simulate the damping behavior of different materials and substrates, financial models, and many other scenarios.

Solitary wave equations like $(1+1)$-dimensional Mikhailov–Novikov–Wang equation (15), RLW equation (16), complex Ginzburg–Landau model [17], and Korteweg and de Vries equations [18] have assembled a lot of interest from researchers. Among them, the most relevant family is KdV equations which also provide a foundation for other models. During 1895, Korteweg and de Vries first modeled the classical KdV equation [18]. These equations are highly nonlinear and describe wave structures in crystal lattice, plasma, water, and density stratified ocean waves, etc., that are explored by many researchers. Heydari et al. observed fractional KdV-burger's equation by discrete Chebyshev polynomials [19], second order difference schemes for time-fractional KdV-burger's is solved by Cen et al. [20], fractional Kaup–Kupershmidt equation is analyzed by Shah et al. [21], Iqbal et al. [22] applied Atangana-Baleanu derivative on fractional Kersten–Krasil'shchik coupled KdV-mKdV system. KdV equations are also used in string theory with continuum limit. Similarly, the study of many physical aspects through KdV equations in quantum field theory,

general relativity, and fluid mechanics are explored in recent studies [23–26]. Crabb et al. observed the complex korteweg-de Vries equation [27], forced korteweg-de Vries equation on critical flow over a hole is solved by Veeresha et al. [28], Yavuz et al. utilized fractional order with Mittag–Leffler on Schrodinger-KdV equation [29], Wang and Mei analyzed [30] KdV and Boussinesq hierarchy with a lax triple.

In the present work, generalized third order time-fractional KdV models are investigated through an extended He-Laplace algorithm. The proposed approach is applied to three KdV models, namely, Korteweg-de Vries-Burgers (KdVB) [31], potential Korteweg-de Vries (p-KdV) [32], and time-fraction dispersive KdV equation [31]. The generalized KdVB equation was proposed by Su and Gardner in 1969 [33] by combining the classical KdV equation [18] with the Burgers equation [34]. General form of KdVB model is

$$\frac{\partial^{\tau}\Upsilon(x,\tau)}{\partial\tau^{\tau}}+\Upsilon(x,\tau)\frac{\partial\Upsilon(x,\tau)}{\partial x}-\rho\frac{\partial^{2}\Upsilon(x,\tau)}{\partial x^{2}}+\sigma\frac{\partial^{3}\Upsilon(x,\tau)}{\partial x^{3}}=0, \tag{1}$$

where x and τ are spatial and temporal variables while Υ is the wave profile, ρ and σ are nonzero real constants, Υ_{xx} is viscous loss, Υ_{xxx} and $\Upsilon\Upsilon_{x}$ are dispersion and convective nonlinearity, respectively. KdVB equation depicts several physical phenomena like the flow of liquids containing gas bubbles, propagation of waves in an elastic tube filled with a viscous fluid, plasma waves, and propagation of bores in shallow water etc.

On the other hand, the p-KdV equation [32] replicates waves on much greater frequency such as tsunami waves. The standard form of P-KdV is

$$\frac{\partial^{\tau}\Upsilon(x,\tau)}{\partial\tau^{\tau}}+\rho\left(\frac{\partial\Upsilon(x,\tau)}{\partial x}\right)^{2}+\sigma\frac{\partial^{3}\Upsilon(x,\tau)}{\partial x^{3}}=0. \tag{2}$$

Here, Υ_{τ} is the evolution term, $(\Upsilon_{x})^{2}$ is the nonlinear term and Υ_{xxx} is the dispersion term. Moreover, x, τ indicate spatial and temporal variables while and Υ is the wave profile, respectively. ρ and σ are nonzero real constants.

Computing the exact or approximate solutions of fractional differential equations (FDEs) is very important in all the mentioned fields, but due to the complex nature of FDEs, the exact solution is not possible in most of the cases. As a result, it is essential to compute approximate solutions through analytical or numerical methods like the fractional natural decomposition method [35], Fourier spectral method [36], Lie symmetry analysis [37], auxiliary function method [38], consistent Riccati expansion method [39], and homotopy perturbation method [40]. For better accuracy while dealing with nonlinear problems, various modifications of HPM are also employed on different equations. A few of these modifications are; HPM coupled with the PSEM method [41], Li-He's modified homotopy perturbation method [42], modified HPM for the solution of parametric cubic-quintic nonconservative duffing oscillator [43], novel homotopy perturbation method with exponential-decay kernel [44], He-Laplace method [45]. The he-Laplace technique combines Laplace transform with classic HPM. This modified algorithm can easily solve nonlinear problems with reasonable accuracy. In the current manuscript, He-Laplace is extended to nonlinear generalized third order time-fractional KdV models. The algorithm is tested against the potential KdV model (high frequency model mostly used for tsunami waves), KdV Burgers model, and dispersive KdV model. In the rest of the manuscript, Sections 2 and 3 present the definitions and general methodology of the He-Laplace algorithm for generalized third-order time-fractional KdV models. Section 4 is showing the convergence and error estimation. The application of the He-Laplace approach to KdV models is in Section 5. Discussion results are presented in Section 6 while the conclusion is in Section 7.

2. Definitions

Definition 1. The Laplace transform $\mathbb{L}$ coupled with the Riemann–Liouville time-fractional integral $\mathbb{I}_{\tau}^{\alpha}$ [46] is described as follows [47]:

$$\mathbb{L}\left[\mathbb{I}_{\tau}^{\alpha}\Upsilon(x,\tau)\right]=s^{-\alpha}\mathbb{L}\left[\Upsilon(x,\tau)\right],\ \zeta-1<\alpha\leq\zeta. \tag{3}$$

Definition 2. The Laplace transform $\mathbb{L}$ coupled with Caputo's time-fractional derivative $\mathbb{D}_{\tau}^{\alpha}$ [46] is described as follows [47]:

$$\mathbb{L}\left[\mathbb{D}_{\tau}^{\alpha}\Upsilon(x,\tau)\right]=s^{\alpha}\mathbb{L}\left[\Upsilon(x,\tau)\right]-\sum_{i=0}^{\zeta-1}s^{\alpha-i-1}\Upsilon^{(\zeta)}(x,0),\ \zeta-1<\alpha\leq\zeta. \tag{4}$$

3. Fundamental Concept of He-Laplace Algorithm for Third-Order Time-Fractional KdV Models

Consider a general third order, time-fractional KdV equation as follows:

$$\mathbb{D}_{\tau}^{\alpha}\left[\Upsilon(x,\tau)\right]+L\left[\Upsilon(x,\tau)\right]+N\left[\Upsilon(x,\tau)\right]-h(x,\tau)=0,\quad x\,\varepsilon\,\Pi,\ \tau>0,\ \zeta-1<\alpha\leq\zeta, \tag{5}$$

that depend on initial conditions

$$\Upsilon^{(\zeta)}(x,0)=\mathscr{J}^{\zeta}, \tag{6}$$

where Υ is an unknown function that has time-fractional derivative $\mathbb{D}_{\tau}^{\alpha}$, $h(x,\tau)$ is a known function with x and τ as space and time variables respectively. Π is the domain of x and L and N are symbols of linear and nonlinear operators, respectively.

Start the procedure by applying Laplace transform on (5), which gives

$$\mathbb{L}\{\mathbb{D}_\tau^\alpha[\Upsilon(x,\tau)]\} + \mathbb{L}\{L[\Upsilon(x,\tau)] + N[\Upsilon(x,\tau)] - h(x,\tau)\} = 0. \quad (7)$$

By using Def. (4), we have

$$\mathbb{L}[\Upsilon(x,\tau)] - \left(\frac{1}{s^\alpha}\right)\sum_{i=0}^{\zeta-1} s^{\alpha-i-1}\Upsilon^{(\zeta)}(x,0) + \left(\frac{1}{s^\alpha}\right)\mathbb{L}\{\mathrm{L}[\Upsilon(x,\tau)] + \mathrm{N}[\Upsilon(x,\tau)] - h(x,\tau)\} = 0. \quad (8)$$

Homotopy of the above-given equation is:

$$\begin{aligned}\mathcal{Q} &= (1-p)\left(\mathbb{L}\{\Upsilon(x,\tau;p)\} - \Upsilon_0(x,\tau)\right)\\ &+ p\left(\mathbb{L}\{\Upsilon(x,\tau;p)\} - \left(\frac{1}{s^\alpha}\right)\sum_{i=0}^{\zeta-1} s^{\alpha-i-1}\Upsilon^{(\zeta)}(x,0) + \left(\frac{1}{s^\alpha}\right)\mathbb{L}\{L[\Upsilon(x,\tau)] + N[\Upsilon(x,\tau)] - h(x,\tau)\}\right),\end{aligned} \quad (9)$$

where $\Upsilon_0(x,\tau)$ represent the initial guess.

By expanding $\Upsilon(x,\tau)$ using Taylor series with regard to p, we get

$$\Upsilon(x,\tau;p) = \sum_{y=1}^{\infty} p^y \Upsilon_y. \quad (10)$$

Substituting the (10) in (9), and after that equating the coefficients of p with identical powers, we acquire the following equation.

The equation at first order:

$$\begin{aligned}&\mathbb{L}\{\Upsilon_1(x,\tau)\} + \Upsilon_0(x,\tau) - \left(\frac{1}{s^\alpha}\right)\sum_{i=0}^{\zeta-1} s^{\alpha-i-1}\Upsilon^{(\zeta)}(x,0) + \left(\frac{1}{s^\alpha}\right)\mathbb{L}\{L[\Upsilon_0(x,\tau)] + N[\Upsilon_0(x,\tau)] - h(x,\tau)\} = 0,\\ &\Upsilon_1^{(\zeta)}(x,0) = \mathcal{J}_1^\zeta,\end{aligned} \quad (11)$$

Implementing inverse Laplace transform leads to

$$\Upsilon_1(x,\tau) + \mathbb{L}^{-1}\left\{\Upsilon_0(x,\tau) - \left(\frac{1}{s^\alpha}\right)\sum_{i=0}^{\zeta-1} s^{\alpha-i-1}\Upsilon^{(\zeta)}(x,0)\right\} + \mathbb{L}^{-1}\left\{\left(\frac{1}{s^\alpha}\right)\mathbb{L}\{L[\Upsilon_0(x,\tau)] + N[\Upsilon_0(x,\tau)] - h(x,\tau)\}\right. = 0, \quad (12)$$

In general, equation at m^{th} order is

$$\begin{aligned}&\mathbb{L}\{\Upsilon_m(x,\tau)\} + \left(\frac{1}{s^\alpha}\right)\mathbb{L}\{L[\Upsilon_{m-1}(x,\tau)] + N[\Upsilon_{m-1}(x,\tau)]\} = 0,\\ &\Upsilon_{m-1}^{(\zeta)}(x,0) = \mathcal{J}_{m-1}^\zeta,\end{aligned} \quad (13)$$

Inverse Laplace transform of the above-given equation is

$$\Upsilon_m(x,\tau) + \mathbb{L}^{-1}\left\{\left(\frac{1}{s^\alpha}\right)\mathbb{L}\{L[\Upsilon_{m-1}(x,\tau)] + N[\mathcal{R}_{m-1}(x,\tau)]\}\right\} = 0, \quad (14)$$

The approximate series solution of the general third order, time-fractional KdV equation is

$$\widetilde{\Upsilon} = \Upsilon_0(x,\tau) + \Upsilon_1(x,\tau) + \Upsilon_2(x,\tau) + \Upsilon_3(x,\tau) + \Upsilon_4(x,\tau) + \ldots. \quad (15)$$

Substituting (15) in (5) gives residual function as follows:

$$\mathbb{R} = \mathbb{D}_\tau^\alpha[\widetilde{\Upsilon}] + L[\widetilde{\Upsilon}] + N[\widetilde{\Upsilon}] - h(x,\tau). \quad (16)$$

4. Convergence Analysis and Error Estimation

4.1. Convergence

Theorem 1. *Let a Banach space $(\mathbb{B}[0,\mathbb{T}], \|.\|)$ has functions $\Upsilon_i(x,\tau)$ and $\Upsilon(x,\tau)$ defined in it. Then, the series solution given in equation (16) converges towards the solution of (5) with constant $\varrho \epsilon$ (0, 1).*

Proof. For the sequence of partial sums $\{c_i\}$ of (16), we have to verify that $c_i(x,\tau)$ is a Cauchy sequence in $(\mathbb{B}[0,\mathbb{T}], \|.\|)$. Consider

$$\begin{aligned}\left\|c_{i+1}(x,\tau)-c_i(x,\tau)\right\| &= \left\|\Upsilon_{i+1}(x,\tau)\right\| \le \varrho\left\|\Upsilon_i(x,\tau)\right\| \\ &\le \varrho^2\left\|\Upsilon_{i-1}(x,\tau)\right\| \le \cdots \le \varrho^{i+1}\left\|\Upsilon_0(x,\tau)\right\|.\end{aligned} \tag{17}$$

By the successive use of triangle inequality on the partial sums c_i and c_j with $i, j \varepsilon \mathbb{N}$ and $i \ge j$, we have

$$\begin{aligned}\left\|c_i-c_j\right\| &= \left\|\left(c_i(x,\tau)-c_{i-1}(x,\tau)\right)+\left(c_{i-1}(x,\tau)-c_{i-2}(x,\tau)\right)+\cdots+\left(c_{j+1}(x,\tau)-c_j(x,\tau)\right)\right\| \\ &\le \left\|c_i(x,\tau)-c_{i-1}(x,\tau)\right\|+\left\|c_{i-1}(x,\tau)-c_{i-2}(x,\tau)\right\|+\cdots+\left\|c_{j+1}(x,\tau)-c_j(x,\tau)\right\|,\end{aligned} \tag{18}$$

Using (17), we get

$$\begin{aligned}\left\|c_i-c_j\right\| &\le \varrho^i\left\|\Upsilon_0(x,\tau)\right\|+\varrho^{i-1}\left\|\Upsilon_0(x,\tau)\right\|+\cdots+\varrho^{j+1}\left\|\Upsilon_0(x,\tau)\right\| \\ &\le \left(\varrho^i+\varrho^{i-1}+\cdots+\varrho^{j+1}\right)\left\|\Upsilon_0(x,\tau)\right\| \\ &\le \varrho^{j+1}\left(\varrho^{i-j-1}+\varrho^{i-j-2}+\cdots+\varrho+1\right)\left\|\Upsilon_0(x,\tau)\right\| \\ &\le \varrho^{j+1}\left(\frac{1-\varrho^{i-j}}{1-\varrho}\right)\left\|\Upsilon_0(x,\tau)\right\|,\end{aligned} \tag{19}$$

Given that $0 < \varrho < 1$, hence, $1-\varrho^{i-j} < 1$. Thus,

$$\left\|c_i-c_j\right\| \le \frac{\varrho^{j+1}}{1-\varrho}\max_{t\in[0,\mathbb{T}]}\left|\Upsilon_0(x,\tau)\right|, \tag{20}$$

Υ_0 is bounded so, it gives

$$\lim_{i,j\longrightarrow\infty}\left\|c_i(x,\tau)-c_j(x,\tau)\right\| = 0. \tag{21}$$

Hence, we have proved that $c_i(x,\tau)$ is a Cauchy sequence in Banach space. Therefore, the series solution given in (15) converges towards the solution of (5). □

4.2. Error Estimation

Theorem 2. *For a third order, time-fractional KdV equation (5), the maximum absolute truncation error of its solution (16) is*

$$\left|\Upsilon(x,\tau)-\sum_{h=0}^{j}\Upsilon_h(x,\tau)\right| \le \frac{\varrho^{j+1}}{1-\varrho}\left\|\Upsilon_0(x,\tau)\right\|. \tag{22}$$

Proof. Equation (20) gives

$$\left\|\Upsilon(x,\tau)-c_j\right\| \le \varrho^{j+1}\left(\frac{1-\varrho^{i-j}}{1-\varrho}\right)\left\|\Upsilon_0(x,\tau)\right\|. \tag{23}$$

Since $0<\varrho<1$, therefore $1-\varrho^{i-j}<1$, which gives

$$\left|\Upsilon(x,\tau)-\sum_{h=0}^{j}\Upsilon_h(x,\tau)\right| \le \frac{\varrho^{j+1}}{1-\varrho}\left\|\Upsilon_0(x,\tau)\right\|. \tag{24}$$

Hence proved. □

5. Solutions of Time-Fractional KdV Models Using He-Laplace Algorithm

Example 1. Consider the time-fractional potential KdV equation

$$\frac{\partial^\alpha\Upsilon(x,\tau)}{\partial\tau^\alpha}+\rho\left(\frac{\partial\Upsilon(x,\tau)}{\partial x}\right)^2+\sigma\frac{\partial^3\Upsilon(x,\tau)}{\partial x^3}=0,\ 0<\alpha\le 1, \tag{25}$$

with initial condition

$$\Upsilon(x,0)=\frac{6\sigma\sqrt{\nu}}{2\rho\sqrt{\sigma}}\tanh\left(\frac{x\sqrt{\nu}}{2\sqrt{\sigma}}\right). \tag{26}$$

The exact solution of p-KdV (25) is

$$\Upsilon(x,\tau)=\frac{6\sigma\sqrt{\nu}}{2\rho\sqrt{\sigma}}\tanh\left(\frac{x\sqrt{\nu}}{2\sqrt{\sigma}}-\frac{\nu\sqrt{\nu}\,\tau}{2\sqrt{\sigma}}\right). \tag{27}$$

Solution 1. Initiating Laplace transform of given p-KdV (25) and then adapting definition (4) gives

$$s^\alpha\mathbb{L}[\Upsilon(x,\tau)]-s^{\alpha-1}\frac{6\sigma\sqrt{\nu}}{2\rho\sqrt{\sigma}}\tanh\left(\frac{x\sqrt{\nu}}{2\sqrt{\sigma}}\right)+\mathbb{L}\left\{\rho\left(\frac{\partial\Upsilon}{\partial x}\right)^2+\sigma\frac{\partial^3\Upsilon}{\partial x^3}\right\}=0. \tag{28}$$

Homotopy of (28) is

$$\mathcal{Q} = (1-p)\left(\mathbb{L}\{\Upsilon(x,\tau)\} - \Upsilon_0(x,\tau)\right) + p\left(\mathbb{L}\{\Upsilon(x,\tau)\} - \left(\frac{1}{s}\right)\frac{6\sigma\sqrt{\nu}}{2\rho\sqrt{\sigma}}\tanh\left(\frac{x\sqrt{\nu}}{2\sqrt{\sigma}}\right) + \left(\frac{1}{s^{\alpha}}\right)\mathbb{L}\left\{\rho\left(\frac{\partial\Upsilon}{\partial x}\right)^2 + \sigma\frac{\partial^3\Upsilon}{\partial x^3}\right\}\right), \tag{29}$$

where, the initial guess $\Upsilon_0(x,\tau)$ is

$$\Upsilon_0(x,\tau) = \frac{6\sigma\sqrt{\nu}}{2\rho\sqrt{\sigma}}\tanh\left(\frac{x\sqrt{\nu}}{2\sqrt{\sigma}}\right). \tag{30}$$

Using (10) and then equalizing the same coefficients of p gives.

Equation at first order:

$$\mathbb{L}\{\Upsilon_1(x,\tau)\} + \Upsilon_0(x,\tau) - \left(\frac{1}{s}\right)\frac{6\sigma\sqrt{\nu}}{2\rho\sqrt{\sigma}}\tanh\left(\frac{x\sqrt{\nu}}{2\sqrt{\sigma}}\right) + \left(\frac{1}{s^{\alpha}}\right)\mathbb{L}\left\{\rho\left(\frac{\partial\Upsilon_0}{\partial x}\right)^2 + \sigma\frac{\partial^3\Upsilon_0}{\partial x^3}\right\} = 0, \quad \Upsilon_1(x,0) = 0, \tag{31}$$

Implementing inverse Laplace transform gives:

$$\Upsilon_1(x,\tau) = \frac{-\tau^{\alpha}\left(\left(3\nu^2\operatorname{sech}^4(\sqrt{\nu}\,x/2\sqrt{\sigma})/2\rho\right) + \left(3\nu^2\tanh^2(\sqrt{\nu}\,x/2\sqrt{\sigma})\operatorname{sech}^2(\sqrt{\nu}\,x/2\sqrt{\sigma})/2\rho\right)\right)}{\Gamma(\alpha+1)}. \tag{32}$$

Equation at second order:

$$\mathbb{L}\{\Upsilon_2(x,\tau)\} + \left(\frac{1}{s^{\alpha}}\right)\mathbb{L}\left\{\rho\left(\frac{\partial\Upsilon_1}{\partial x}\right)^2 + \sigma\frac{\partial^3\Upsilon_1}{\partial x^3}\right\} = 0, \quad \Upsilon_2(x,0) = 0. \tag{33}$$

Solution at second order:

$$\Upsilon_2(x,\tau) = -\frac{12\nu^{7/2}\tau^{2\alpha}\sinh^4(\sqrt{\nu}\,x/2\sqrt{\sigma})\operatorname{csch}^3(\sqrt{\nu}\,x/\sqrt{\sigma})}{\rho\sqrt{\sigma}\Gamma(2\alpha+1)}. \tag{34}$$

Equation at third order:

$$\mathbb{L}\{\Upsilon_3(x,\tau)\} + \left(\frac{1}{s^{\alpha}}\right)\mathbb{L}\left\{\rho\left(\frac{\partial\Upsilon_2}{\partial x}\right)^2 + \sigma\frac{\partial^3\Upsilon_2}{\partial x^3}\right\} = 0, \quad \Upsilon_3(x,0) = 0, \tag{35}$$

Solution at third order:

$$\Upsilon_3(x,\tau) = -3\nu^5\tau^{3\alpha}\operatorname{sech}^6\left(\frac{\sqrt{\nu}\,x}{2\sqrt{\sigma}}\right) \frac{\left(\Gamma(\alpha+1)^2(-14\cosh(\sqrt{\nu}\,x/\sqrt{\sigma}) + \cosh(2\sqrt{\nu}\,x/\sqrt{\sigma}) + 9) + 6\Gamma(2\alpha+1)(\cosh(\sqrt{\nu}\,x/\sqrt{\sigma}) - 1)\right)}{16\rho\sigma\Gamma(\alpha+1)^2\Gamma(3\alpha+1)}. \tag{36}$$

Obtained approximate series solution of (25) is

$$\widetilde{\Upsilon} = \Upsilon_0(x,\tau) + \Upsilon_1(x,\tau) + \Upsilon_2(x,\tau) + \Upsilon_3(x,\tau) + \Upsilon_4(x,\tau) + \ldots. \tag{37}$$

Residual function '$\mathbb{R}$' of (25) is

$$\mathbb{R} = \frac{\partial^{\alpha}\widetilde{\Upsilon}}{\partial\tau^{\alpha}} + \rho\left(\frac{\partial\widetilde{\Upsilon}}{\partial x}\right)^2 + \sigma\frac{\partial^3\Upsilon}{\partial x^3}. \tag{38}$$

Example 2. Consider the time-fractional dispersive KdV equation

$$\frac{\partial^{\alpha}\Upsilon(x,\tau)}{\partial\tau^{\alpha}}+\Upsilon(x,\tau)\frac{\partial\Upsilon(x,\tau)}{\partial x}+\frac{1}{2}\frac{\partial^{3}\Upsilon(x,\tau)}{\partial x^{3}}=0,\ 0<\alpha\leq 1, \tag{39}$$

associated with initial condition

$$\Upsilon(x,0)=6\rho^{2}\sec h^{2}(\rho x). \tag{40}$$

The exact solution is

$$\Upsilon(x,\tau)=6\rho^{2}\sec h^{2}\left(\rho x-2\rho^{3}\tau\right). \tag{41}$$

Solution 2. Procedure given in Section 3 leads to:

The initial guess $\Upsilon_0(x,\tau)$ that is

$$\Upsilon_0(x,\tau)=6\rho^{2}\sec h^{2}(\rho x). \tag{42}$$

Equation at first order:

$$\mathbb{L}\{\Upsilon_1(x,\tau)\}+\Upsilon_0(x,\tau)-\left(\frac{1}{s}\right)6\rho^{2}\sec h^{2}(\rho x)+\left(\frac{1}{s^{\alpha}}\right)\mathbb{L}\left\{\Upsilon_0(x,\tau)\frac{\partial\Upsilon_0(x,\tau)}{\partial x}+\frac{1}{2}\frac{\partial^{3}\Upsilon_0(x,\tau)}{\partial x^{3}}\right\}=0,$$
$$\Upsilon_1(x,0)=0, \tag{43}$$

Solution at first order

$$\Upsilon_1(x,\tau)=-\frac{\tau^{\alpha}\left(-24\rho^{5}\tanh(\rho x)\sec h^{4}(\rho x)-24\rho^{5}\tanh^{3}(\rho x)\sec h^{2}(\rho x)\right)}{\Gamma(\alpha+1)}. \tag{44}$$

Equation at the second order:

$$\mathbb{L}\{\Upsilon_2(x,\tau)\}+\left(\frac{1}{s^{\alpha}}\right)\mathbb{L}\left\{\Upsilon_1(x,\tau)\frac{\partial\Upsilon_1(x,\tau)}{\partial x}+\frac{1}{2}\frac{\partial^{3}\Upsilon_1(x,\tau)}{\partial x^{3}}\right\}=0,$$
$$\Upsilon_2(x,0)=0, \tag{45}$$

Solution at the second order:

$$\Upsilon_2(x,\tau)=\frac{48\rho^{8}\tau^{2\alpha}(\cosh(2\rho x)-2)\sec h^{4}(\rho x)}{\Gamma(2\alpha+1)}. \tag{46}$$

Equation at third order:

$$\mathbb{L}\{\Upsilon_3(x,\tau)\}+\left(\frac{1}{s^{\alpha}}\right)\mathbb{L}\left\{\Upsilon_2(x,\tau)\frac{\partial\Upsilon_2(x,\tau)}{\partial x}+\frac{1}{2}\frac{\partial^{3}\Upsilon_2(x,\tau)}{\partial x^{3}}\right\}=0,$$
$$\Upsilon_3(x,0)=0, \tag{47}$$

Solution at third order:

$$\Upsilon_3(x,\tau)=48\rho^{11}\tau^{3\alpha}\tanh(\rho x)\sec h^{6}(\rho x)$$
$$\frac{\left(\Gamma(\alpha+1)^{2}(-32\cosh(2\rho x)+\cosh(4\rho x)+39)+12\Gamma(2\alpha+1)(\cosh(2\rho x)-2)\right)}{\Gamma(\alpha+1)^{2}\Gamma(3\alpha+1)}, \tag{48}$$

Approximate series solution of (39) by the He-Laplace algorithm can be observed by

$$\widetilde{\Upsilon}=\Upsilon_0(x,\tau)+\Upsilon_1(x,\tau)+\Upsilon_2(x,\tau)+\Upsilon_3(x,\tau)+\Upsilon_4(x,\tau)+\ldots. \tag{49}$$

Residual function '$\mathbb{R}$' of (39) is

$$\mathbb{R}=\frac{\partial^{\alpha}\widetilde{\Upsilon}}{\partial\tau^{\alpha}}+\widetilde{\Upsilon}\frac{\partial\widetilde{\Upsilon}}{\partial x}+\frac{1}{2}\frac{\partial^{3}\widetilde{\Upsilon}}{\partial x^{3}}. \tag{50}$$

Example 3. Consider the time-fractional KdV Burgers equation

$$\frac{\partial^{\alpha}\Upsilon(x,\tau)}{\partial\tau^{\alpha}}+\Upsilon(x,\tau)\frac{\partial\Upsilon(x,\tau)}{\partial x}-\rho\frac{\partial^{2}\Upsilon(x,\tau)}{\partial x^{2}}+\frac{1}{2}\frac{\partial^{3}\Upsilon(x,\tau)}{\partial x^{3}}=0,0<\alpha\leq 1, \tag{51}$$

that has initial condition

$$\Upsilon(x,0)=\frac{6\rho}{25^{2}}\left(2-2\tanh\left(\frac{\rho x}{5}\right)+\sec h^{2}\left(\frac{\rho x}{5}\right)\right). \tag{52}$$

The exact solution of KdV Burgers equation is

$$\Upsilon(x,\tau)=\frac{6\rho}{25^{2}}\left(2-2\tanh\left(\frac{\rho x}{5}-\frac{12\rho^{3}\tau}{125}\right)+\sec h^{2}\left(\frac{\rho x}{5}-\frac{12\rho^{3}\tau}{125}\right)\right). \tag{53}$$

Solution 3. Procedure in Section 3 gives:

The initial guess $\Upsilon_0(x,\tau)$ that is

$$\Upsilon_0(x,\tau) = \frac{6\rho}{25^2}\left(2 - 2\tanh\left(\frac{\rho x}{5}\right) + \sec h^2\left(\frac{\rho x}{5}\right)\right). \tag{54}$$

Equation at first order:

$$\begin{aligned} &\mathbb{L}\{\Upsilon_1(x,\tau)\} + \Upsilon_0(x,\tau) - \left(\frac{1}{s}\right)\frac{6\rho}{25^2}\left(2 - 2\tanh\left(\frac{\rho x}{5}\right) + \sec h^2\left(\frac{\rho x}{5}\right)\right) + \left(\frac{1}{s^\alpha}\right) \\ &\mathbb{L}\left\{\Upsilon_0(x,\tau)\frac{\partial \Upsilon_0(x,\tau)}{\partial x} - \rho\frac{\partial^2 \Upsilon_0(x,\tau)}{\partial x^2} + \frac{1}{2}\frac{\partial^3 \Upsilon_0(x,\tau)}{\partial x^3}\right\} = 0, \\ &\Upsilon_1(x,0) = 0, \end{aligned} \tag{55}$$

Equation at second order:

$$\begin{aligned} &\mathbb{L}\{\Upsilon_2(x,\tau)\} + \left(\frac{1}{s^\alpha}\right)\mathbb{L}\left\{\Upsilon_1(x,\tau)\frac{\partial \Upsilon_1(x,\tau)}{\partial x} - \rho\frac{\partial^2 \Upsilon_1(x,\tau)}{\partial x^2} + \frac{1}{2}\frac{\partial^3 \Upsilon_1(x,\tau)}{\partial x^3}\right\} = 0, \\ &\Upsilon_2(x,0) = 0, \end{aligned} \tag{56}$$

Equation at third order:

$$\begin{aligned} &\mathbb{L}\{\Upsilon_3(x,\tau)\} + \left(\frac{1}{s^\alpha}\right)\mathbb{L}\left\{\Upsilon_2(x,\tau)\frac{\partial \Upsilon_2(x,\tau)}{\partial x} - \rho\frac{\partial^2 \Upsilon_2(x,\tau)}{\partial x^2} + \frac{1}{2}\frac{\partial^3 \Upsilon_2(x,\tau)}{\partial x^3}\right\} = 0, \\ &\Upsilon_3(x,0) = 0, \end{aligned} \tag{57}$$

After taking inverse Laplace transform of these problems the approximate series is

$$\tilde{\Upsilon} = \Upsilon_0(x,\tau) + \Upsilon_1(x,\tau) + \Upsilon_2(x,\tau) + \Upsilon_3(x,\tau) + \Upsilon_4(x,\tau) + \ldots. \tag{58}$$

Residual errors of (51) can be examined by the following equation:

$$\mathbb{R} = \frac{\partial^\alpha \tilde{\Upsilon}}{\partial \tau^\alpha} + \tilde{\Upsilon}\frac{\partial \tilde{\Upsilon}}{\partial x} - \rho\frac{\partial^2 \tilde{\Upsilon}}{\partial x^2} + \frac{1}{2}\frac{\partial^3 \tilde{\Upsilon}}{\partial x^3}. \tag{59}$$

6. Results and Discussion

In this paper, several third order KdV models, KdV-Burger's, time-fractional dispersive KdV, and potential-KdV models are examined at both fractional and integral orders. The solution and analysis of these models are depicted in graphical and tabular form. For this purpose, an efficient semianalytical technique, He-Laplace method is utilized. For Example 1, the convergence of the p-KdV equation for fractional parameter $\alpha = 1$, can be examined from Table 1. Solutions at third, sixth, and ninth iterations are compared. Increasing iterations by using the He-Laplace algorithm decrease in errors is observed. Table 2 expressed the residual errors calculated by residual function (39) at $\alpha = 0.18$, 0.44, 0.76, and 0.92. This table indicates that as the value of α approaches 1, the errors decline. 3-D Figure 1 demonstrates the solutions and errors in graphical form at $\alpha = 1$. To illustrate the nature of α on surface waves throughout the domain, 2-D diagrams (Figure 2) and (Figure 3) are plotted. Figure 2 shows that at a fixed time, increasing the value of the fractional parameter reduces water level for $(0.0 < x < 0.4)$ whereas it increases the level at $(x > 0.4)$. On the other hand, Figure 3 reveals that increase in values of α at fixed x increases the water level. Figure 4 is the effect of the constant parameter ν on the velocity profile which shows that increasing value of ν increases the velocity profile.

Table 3 of Example 2 displays the comparison between errors obtained by the modified generalized Mittag–Leffler function method (MGMLFM) and the He-Laplace method. It is concluded that the He-Laplace method shows better

Table 1: Absolute errors at different iterations in Example 1 using He-laplace method when $\rho = \sigma = 1$ and $\nu = 0.8$.

x	τ	$\lvert\Upsilon(x,\tau) - \widetilde{\Upsilon}_3(x,\tau)\rvert$	$\lvert\Upsilon(x,\tau) - \widetilde{\Upsilon}_6(x,\tau)\rvert$	$\lvert\Upsilon(x,\tau) - \widetilde{\Upsilon}_9(x,\tau)\rvert$
	0.1	8.42×10^{-8}	9.83×10^{-13}	4.44×10^{-16}
	0.3	6.48×10^{-6}	2.15×10^{-9}	3.82×10^{-13}
3	0.5	4.69×10^{-5}	7.67×10^{-8}	6.43×10^{-11}
	0.7	1.67×10^{-4}	8.05×10^{-7}	1.89×10^{-9}
	0.9	4.15×10^{-4}	4.64×10^{-6}	2.37×10^{-8}
	0.1	5.60×10^{-8}	2.44×10^{-14}	0.
	0.3	4.64×10^{-6}	5.94×10^{-11}	1.55×10^{-14}
5	0.5	3.66×10^{-5}	2.34×10^{-9}	2.64×10^{-12}
	0.7	1.44×10^{-4}	2.71×10^{-8}	7.73×10^{-11}
	0.9	4.03×10^{-4}	1.73×10^{-7}	9.66×10^{-10}
	0.1	1.10×10^{-8}	1.55×10^{-14}	4.44×10^{-16}
	0.3	9.16×10^{-7}	3.32×10^{-11}	0.
7	0.5	7.28×10^{-6}	1.20×10^{-9}	7.94×10^{-14}
	0.7	2.87×10^{-5}	1.28×10^{-8}	2.41×10^{-12}
	0.9	8.10×10^{-5}	7.53×10^{-8}	3.11×10^{-11}

Table 2: He-laplace error in Example 1 at different values of α when $\rho = \sigma = 1$, $\nu = 0.8$ and $x = 20$.

τ	$\alpha = 0.18$	$\alpha = 0.44$	$\alpha = 0.76$	$\alpha = 0.92$
0.1	1.60×10^{-9}	3.19×10^{-11}	1.08×10^{-13}	5.00×10^{-15}
0.4	5.58×10^{-9}	6.73×10^{-10}	2.11×10^{-11}	2.94×10^{-12}
0.7	9.24×10^{-9}	2.30×10^{-9}	1.77×10^{-10}	3.86×10^{-11}
1.0	1.27×10^{-8}	5.05×10^{-9}	6.87×10^{-10}	1.99×10^{-10}
1.3	1.61×10^{-8}	9.01×10^{-9}	1.86×10^{-9}	6.66×10^{-10}

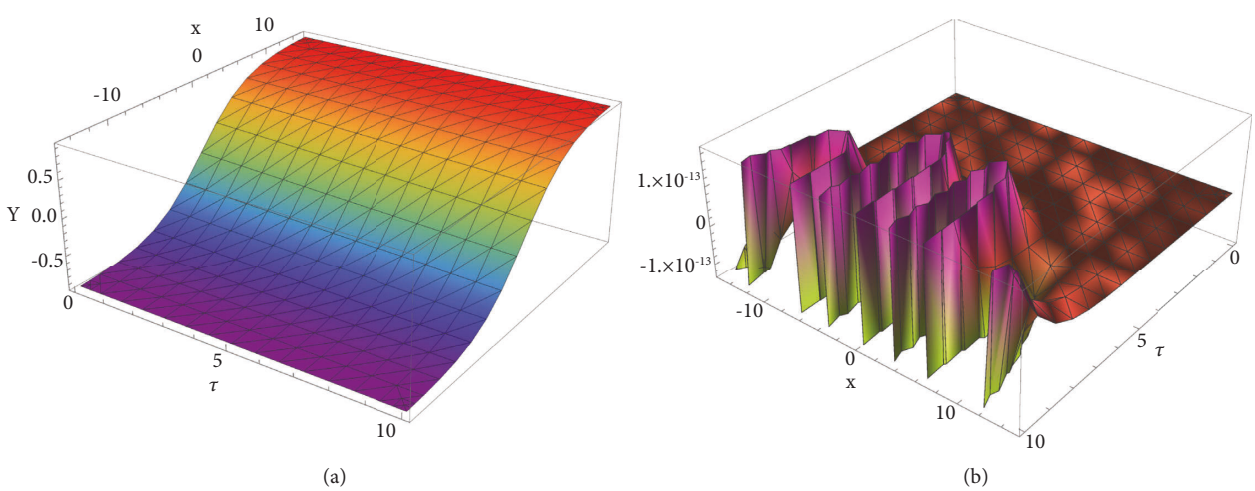

Figure 1: 3D plot of solution and error in Example 1, when $\alpha = 1$, $\rho = \sigma = 1$ and $\nu = 0.1$. (a) Solution. (b) Error.

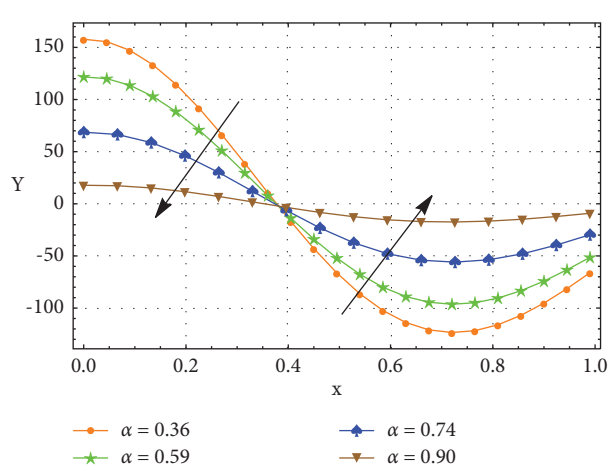

Figure 2: Effect of α on wave profile in Example 1, when $\rho = \sigma = \nu = 1$ and $\tau = 3$.

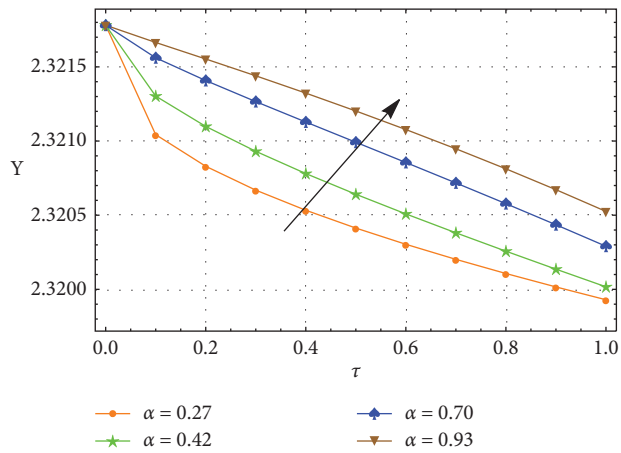

Figure 3: Evaluation of water surface level in Example 1 at different values of α with $\rho = \sigma = 1$, $\nu = 0.6$ and $x = 10$.

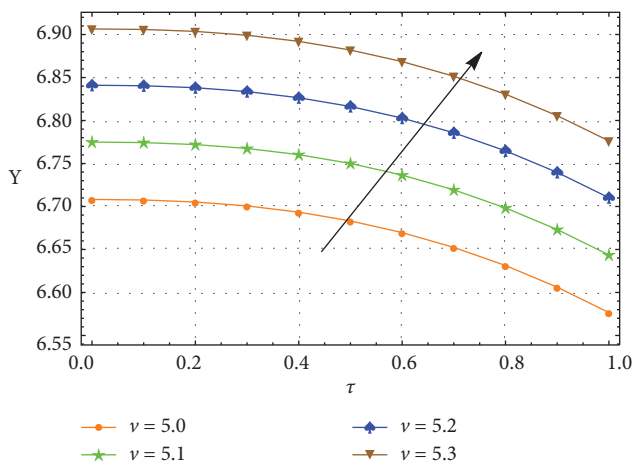

Figure 4: Effect of ν on the solution in Example 1 when $\alpha = 0.5$, $\rho = \sigma = 1$ and $x = 7$.

Table 3: Comparison of He-laplace with MGMLFM in Example 2 when $\alpha = 1$ and $x = 30$.

ρ	τ	He-laplace solution	He-laplace error	MGMLFM error [48]
0.1	5	0.0006038	3.66×10^{-17}	4.15×10^{-9}
	15	0.0006283	2.69×10^{-14}	3.91×10^{-8}
	25	0.0006538	5.79×10^{-13}	1.12×10^{-7}
0.01	5	0.0005490	2.69×10^{-20}	7.58×10^{-14}
	15	0.0005490	9.15×10^{-20}	6.82×10^{-13}
	25	0.0005498	4.61×10^{-20}	1.89×10^{-12}
0.001	5	0.0000059	7.38×10^{-22}	8.47×10^{-22}
	15	0.0000059	5.23×10^{-22}	4.23×10^{-21}
	25	0.0000059	2.07×10^{-22}	1.52×10^{-20}

Table 4: He-laplace errors at different values of α when $\rho = 0.18$ and $x = 15$ in Example 2.

τ	$\alpha = 0.27$	$\alpha = 0.45$	$\alpha = 0.77$	$\alpha = 0.97$
0.1	1.40×10^{-14}	9.89×10^{-16}	2.65×10^{-18}	1.35×10^{-20}
0.2	3.58×10^{-14}	4.71×10^{-15}	3.83×10^{-17}	5.69×10^{-19}
0.3	6.20×10^{-14}	1.17×10^{-14}	1.82×10^{-16}	4.18×10^{-18}
0.4	9.16×10^{-14}	2.24×10^{-14}	5.52×10^{-16}	1.70×10^{-17}
0.5	1.23×10^{-13}	3.71×10^{-14}	1.30×10^{-15}	5.04×10^{-17}

results in terms of accuracy as compared with other methods. Table 4 indicates that as the quantity of fractional parameter rises, error reduces. Figure 5 presents the solution and error plots in 3-D format whereas, Figure 6 is the 2-D representation of effect of α on water waves profile at a certain time. It can be seen from Figure 7 that as α increases throughout the domain, wave profile decreases. Moreover, Figure 8 conveys that the increment in the value of constant parameter ρ decreases the velocity profile.

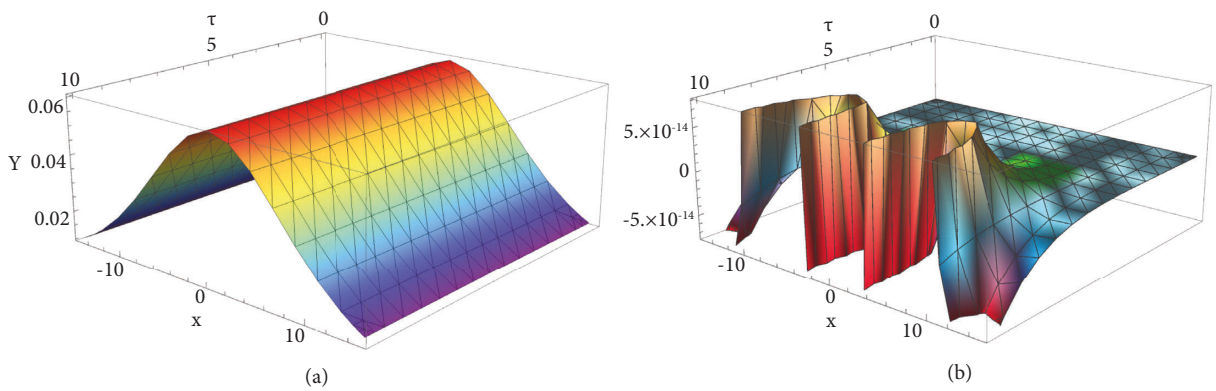

Figure 5: 3D plot of solution and error in Example 2 when $\alpha = 1$ and $\rho = 0.1$. (a) Solution. (b) Error.

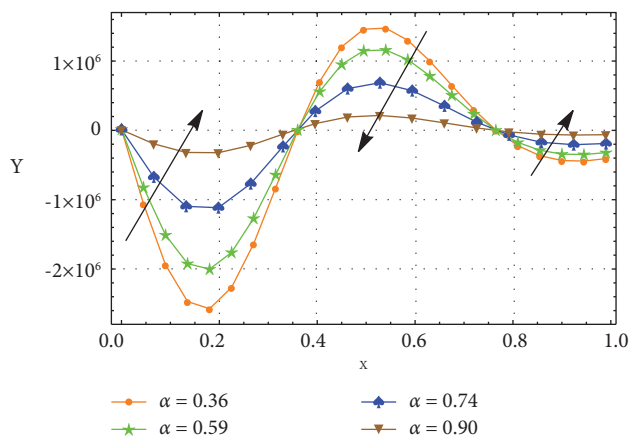

Figure 6: Effect of fractional parameter α on the wave profile in Example 2 when $\rho = 1$ and $\tau = 3$.

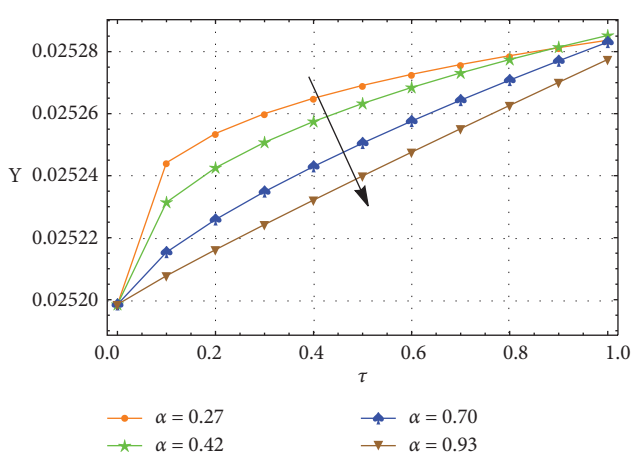

Figure 7: Evaluation of water surface level in Example 2 at different values of α when $\rho = 0.1$ and $x = 10$.

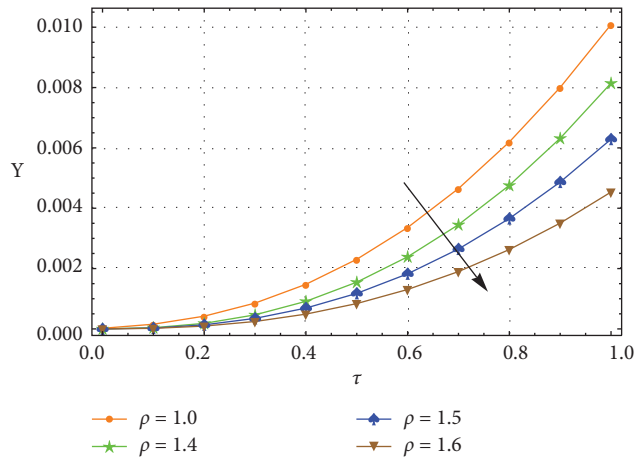

Figure 8: Effect of ρ on the solution profile in Example 2 when $\alpha = 0.5$ and $x = 7$.

Table 5: Comparison of He-laplace algorithm with MGMLFM in Example 3, when $\alpha = 1$ and $x = 30$.

ρ	τ	He-laplace solution	He-laplace error	MGMLFM error [48]
0.1	5	0.0039324	0.	1.10×10^{-9}
	15	0.0039375	$8.67 \times 10^{-}$	9.92×10^{-9}
	25	0.0039425	0.	2.76×10^{-8}
0.01	5	0.0000690	0.	1.52×10^{-17}
	15	0.0000690	0.	1.37×10^{-16}
	25	0.0000690	0.	3.81×10^{-16}
0.001	5	0.0000007	0.	1.05×10^{-22}
	15	0.0000007	0.	1.05×10^{-22}
	25	0.0000007	0.	0.

Table 6: He-laplace error in Example 3 at different values of α when $\rho = 0.5$ and $x = 10$.

τ	$\alpha = 0.27$	$\alpha = 0.53$	$\alpha = 0.77$	$\alpha = 0.97$
0.1	4.68×10^{-12}	5.24×10^{-14}	3.62×10^{-16}	2.05×10^{-18}
0.2	1.19×10^{-11}	3.29×10^{-13}	5.21×10^{-15}	3.90×10^{-17}
0.3	2.06×10^{-11}	9.63×10^{-13}	2.48×10^{-14}	2.74×10^{-16}
0.4	3.04×10^{-11}	2.06×10^{-12}	7.52×10^{-14}	1.11×10^{-15}
0.5	4.11×10^{-11}	3.72×10^{-12}	1.77×10^{-13}	3.28×10^{-15}

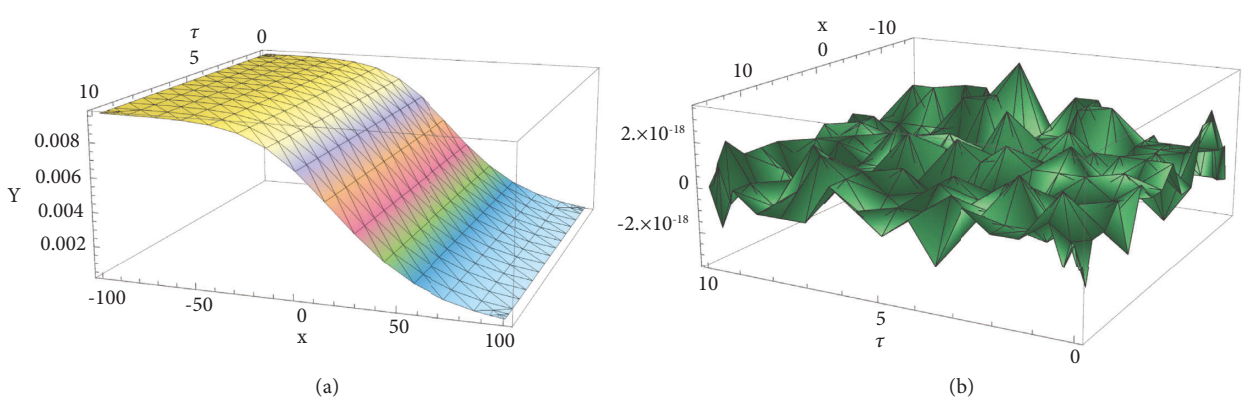

Figure 9: 3D plot of solution and error in Example 3 when $\alpha = 1$ and $\rho = 0.1$. (a) Solution. (b) Error.

In Example 3, the efficiency of the He-Laplace algorithm over other methods is depicted in Table 5. Moreover, Table 6 displays residual errors of the KdVB equation at various α. Figure 9 depicts the approximate solution and absolute error. Figure 10 shows the behaviour of waves at different values of the fractional parameter for a fixed time. At a

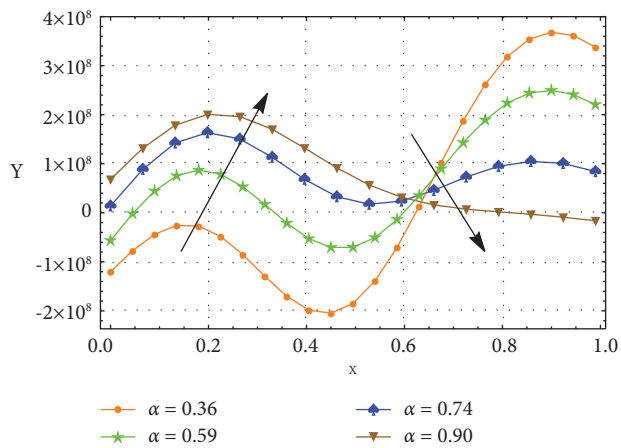

Figure 10: Effect of distinct values of α on wave profile in Example 3 when $\rho = 5$ and $\tau = 3$.

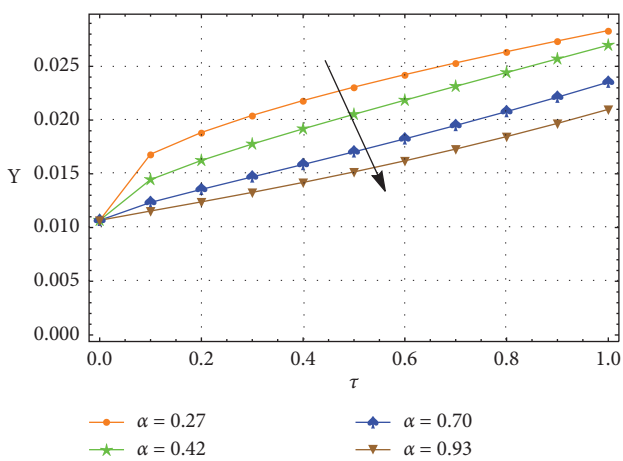

Figure 11: Evaluation of water surface level in Example 3 at different values of α when $\rho = 1.5$ and $x = 10$.

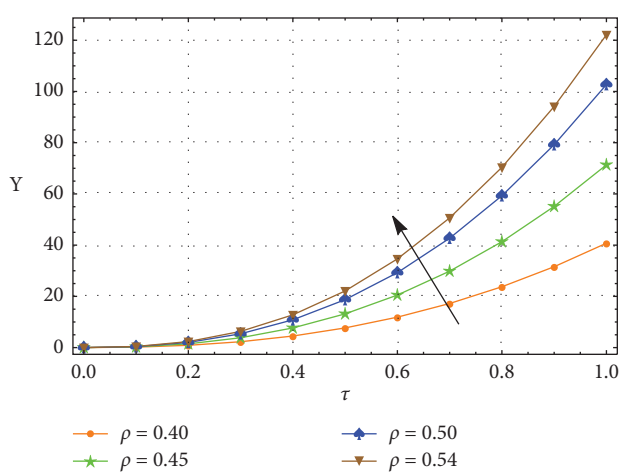

Figure 12: Effect of ρ on solution profile in Example 3 at $\alpha = 0.5$ and $x = 7$.

certain value of a spatial variable, by boosting α the water waves drop (see Figure 11). Also, from Figure 12 we can observe that with higher values of the constant parameter ρ, velocity profile elevates.

7. Conclusion

The focus of this study is to solve and analyze third-order time-fractional KdV models of three different kinds. This investigation can assist researchers to illustrate complex, fractional, and nonlinear real-world problems effectively. In this regard, p-KdV, KdVB, and KdV equations are considered. A highly efficient technique, the He-Laplace method, which is the combination of the homotopy perturbation method (HPM) and Laplace transform, is adapted for solution purpose. Approximate solutions and residual errors are depicted in form of 3-D graphs. The effect of fractional parameter α on wave profile is shown in graphical and tabular form. The convergence of the model is verified through tabular results. With an increase in the number of iterations, series form solutions converge to the analytical solution. Moreover, the reliability of the method is confirmed through comparison with existing results in the literature. The he-Laplace algorithm proved to be an effective technique in solving specified KdV models with least errors and enhanced series solutions.

Data Availability

All the data is within the manuscript.

Conflicts of Interest

The authors declare that they have no conflicts of interest.

References

[1] M. Arif, P. Kumam, W. Kumam, I. Khan, and M. Ramzan, "A fractional model of casson fluid with ramped wall temperature: engineering applications of engine oil," *Computational and Mathematical Methods*, vol. 3, no. 6, may 2021.

[2] M. Cai, G. Em Karniadakis, and C. Li, "Fractional SEIR model and data-driven predictions of COVID-19 dynamics of omicron variant," *Chaos: An Interdisciplinary Journal of Nonlinear Science*, vol. 32, no. 7, Article ID 071101, jul 2022.

[3] Y. Li, M. Peng, T. He, X. Tian, and K. Liao, "A fractional dual-phase-lag generalized thermoelastic model of ultrashort pulse laser ablation with variable thermal material properties, vaporization and plasma shielding," *International Journal of Thermal Sciences*, vol. 177, Article ID 107556, 2022.

[4] Y. Wang, X. He, L. Zhang et al., "A novel fractional time-delayed grey Bernoulli forecasting model and its application for the energy production and consumption prediction," *Engineering Applications of Artificial Intelligence*, vol. 110, Article ID 104683, 2022.

[5] I. L. Y. A. S. Khan, A. M. Alqahtani, A. R. S. H. A. D. Khan, D. O. L. A. T. Khan, A. H. Ganie, and G. Ali, "New results of

fractal fractional model of drilling nanoliquids with clay nanoparticles," *Fractals*, vol. 30, no. 1, jan 2022.

[6] M. Kalidass, S. Zeng, and M. Yavuz, "Stability of fractional-order quasi-linear impulsive integro-differential systems with multiple delays," *Axioms*, vol. 11, no. 7, p. 308, 2022.

[7] L. Joseph, "Mémoire sur quelques questions de géométrie et de mécanique, et sur un nouveau genre de calcul pour résoudre ces questions," *Journal de l'école Polytechnique*, 1832.

[8] K. S. Miller and B. Ross, *An Introduction to the Fractional Calculus and Fractional Differential Equations*, Wiley, Hoboken, NJ, USA, 1993.

[9] M. Caputo, *Elasticita e dissipazione*, Zanichelli, Bologna, Italy, 1969.

[10] B. Riemann, "Versuch einer allgemeinen auffassung der integration und differentiation," *Gesammelte Werke*, vol. 62, p. 1876, 1876.

[11] M. A. Abdou, S. Owyed, A. Abdel-Aty, B. M. Raffah, and S. Abdel-Khalek, "Optical soliton solutions for a space-time fractional perturbed nonlinear Schrödinger equation arising in quantum physics," *Results in Physics*, vol. 16, Article ID 102895, 2020.

[12] S. Rashid, R. Ashraf, and Z. Hammouch, "New generalized fuzzy transform computations for solving fractional partial differential equations arising in oceanography," *Journal of Ocean Engineering and Science*, 2021.

[13] B. Keith, U. Khristenko, and B. Wohlmuth, "A fractional PDE model for turbulent velocity fields near solid walls," *Journal of Fluid Mechanics*, vol. 916, p. A21, apr 2021.

[14] F. S. Khan, M. Sultana, M. Khalid, F. Zaidi, and K. Nonlaopon, "Forecasting the behaviour of fractional black-scholes option pricing equation by laplace perturbation iteration algorithm," *Alexandria Engineering Journal*, vol. 62, pp. 85–97, jan 2023.

[15] S. T. Demiray and U. Bayrakci, "A study on the solutions of (1+1)-dimensional mikhailov-novikov-wang equation," *Mathematical Modelling and Numerical Simulation with Applications*, vol. 2, no. 5, pp. 1–8, 2022.

[16] S. Pak, "Solitary wave solutions for the RLW equation by he's semi inverse method," *International Journal of Nonlinear Sciences and Numerical Stimulation*, vol. 10, no. 4, 2009.

[17] M. A. Isah and A. Yokuş, "The investigation of several soliton solutions to the complex ginzburg-landau model with kerr law nonlinearity," *Mathematical Modelling and Numerical Simulation with Applications*, vol. 2, no. 3, pp. 147–163, 2022.

[18] D. J. Korteweg and G. de Vries, "XLI. *On the change of form of long waves advancing in a rectangular canal, and on a new type of long stationary waves*," *The London, Edinburgh, and Dublin Philosophical Magazine and Journal of Science*, vol. 39, no. 240, pp. 422–443, may 1895.

[19] M. H. Heydari, Z. Avazzadeh, and C. Cattani, "Discrete Chebyshev polynomials for nonsingular variable-order fractional KdV burger's equation," *Mathematical Methods in the Applied Sciences*, vol. 44, no. 2, pp. 2158–2170, sep 2020.

[20] D. Cen, Z. Wang, and Y. Mo, "Second order difference schemes for time-fractional KdV-burgers' equation with initial singularity," *Applied Mathematics Letters*, vol. 112, Article ID 106829, 2021.

[21] N. A. Shah, Y. S. Hamed, K. M. Abualnaja, J.-D. Chung, R. Shah, and A. Khan, "A comparative analysis of fractional-order kaup-kupershmidt equation within different operators," *Symmetry*, vol. 14, no. 5, p. 986, may 2022.

[22] N. Iqbal, T. Botmart, W. W. Mohammed, and A. Ali, "Numerical investigation of fractional-order kersten-krasil'shchik coupled KdV-mKdV system with atangana/baleanu derivative," *Advances in Continuous and Discrete Models*, vol. 2022, no. 1, p. 37, 2022.

[23] S. A. El-Tantawy, A. H. Salas, and W. Albalawi, "New localized and periodic solutions to a korteweg-de vries equation with power law nonlinearity: applications to some plasma models," *Symmetry*, vol. 14, no. 2, p. 197, jan 2022.

[24] A. Hyder and A. H. Soliman, "Analytical manner for abundant stochastic wave solutions of extended KdV equation with conformable differential operators," *Mathematical Methods in the Applied Sciences*, vol. 45, no. 14, pp. 8600–8612, mar 2021.

[25] K. Anna and P. Rozmej, "The Only True (2+1)-dimensional Nonlocal Kdv, Fifth-Order Kdv, and gardner Equations Derived from the Ideal Fluid Model," 2022, https://arxiv.org/abs/2206.08964.

[26] R. Alhami and M. Alquran, "Extracted different types of optical lumps and breathers to the new generalized stochastic potential-KdV equation via using the cole-hopf transformation and hirota bilinear method," *Optical and Quantum Electronics*, vol. 54, no. 9, p. 553, jul 2022.

[27] M. Crabb and N. Akhmediev, "Complex korteweg-de vries equation: a deeper theory of shallow water waves," *Physical Review A*, vol. 103, no. 2, Article ID 022216, feb 2021.

[28] P. Veeresha, M. Yavuz, and C. Baishya, "A computational approach for shallow water forced korteweg-de vries equation on critical flow over a hole with three fractional operators," *An International Journal of Optimization and Control: Theories & Applications*, vol. 11, no. 3, pp. 52–67, dec 2021.

[29] M. Yavuz, T. A. Sulaiman, A. Yusuf, and T. Abdeljawad, "The Schrödinger-KdV equation of fractional order with mittag-leffler nonsingular kernel," *Alexandria Engineering Journal*, vol. 60, no. 2, pp. 2715–2724, apr 2021.

[30] X. Wang and J.-Q. Mei, "On the generalized KdV hierarchy and boussinesq hierarchy with lax triple," *Journal of Nonlinear Mathematical Physics*, vol. 28, no. 3, p. 337, 2021.

[31] K. M. Saad, Al, A. K. Alomari, D. Baleanu, and J. F. Gómez-Aguilar, "On exact solutions for time-fractional korteweg-de vries and korteweg-de vries-burger's equations using homotopy analysis transform method," *Chinese Journal of Physics*, vol. 63, pp. 149–162, feb 2020.

[32] T. Ak and S. Dhawan, "A practical and powerful approach to potential KdV and benjamin equations," *Beni-Suef University Journal of Basic and Applied Sciences*, vol. 6, no. 4, pp. 383–390, dec 2017.

[33] C. H. Su and C. S. Gardner, "Korteweg-de vries equation and generalizations. III. derivation of the korteweg-de vries equation and burgers equation," *Journal of Mathematical Physics*, vol. 10, no. 3, pp. 536–539, mar 1969.

[34] J. M. Burgers, "Application of a model system to illustrate some points of the statistical theory of free turbulence," in *Selected Papers of J. M. Burgers*Springer, Dordrecht, Netherlands, 1995.

[35] P. Veeresha, D. G Prakasha, and J. Singh, "Solution for fractional forced KdV equation using fractional natural decomposition method," *AIMS Mathematics*, vol. 5, no. 2, pp. 798–810, 2020.

[36] C. Han, Y. U.-L. A. N. Wang, and Z. Y. Li, "Numerical solutions of space fractional variable-coefficient kdvmodified kdv equation by fourier spectral method," *Fractals*, vol. 29, no. 8, 2021.

[37] B. Ghanbari, S. Kumar, M. Niwas, and D. Baleanu, "The lie symmetry analysis and exact Jacobi elliptic solutions for the kawahara KdV type equations," *Results in Physics*, vol. 23, Article ID 104006, 2021.

[38] L. Zada, R. Nawaz, K. S. Nisar et al., "New approximate-analytical solutions to partial differential equations via auxiliary function method," *Partial Differential Equations in Applied Mathematics*, vol. 4, Article ID 100045, 2021.

[39] R. M. El-Shiekh and M. Gaballah, "New analytical solitary and periodic wave solutions for generalized variable-coefficients modified KdV equation with external-force term presenting atmospheric blocking in oceans," *Journal of Ocean Engineering and Science*, vol. 7, no. 4, pp. 372–376, aug 2022.

[40] D. D. Ganji, N. Jamshidi, and Z. Z. Ganji, "Hpm and vim methods for finding the exact solutions of the nonlinear dispersive equations and seventh-order sawada–kotera equation," *International Journal of Modern Physics B*, vol. 23, pp. 39–52, 2009.

[41] U. Filobello-Nino, H. Vazquez-Leal, V. M. Tlapa-Carrera, V. M. Jimenez-Fernandez, M. A. Sandoval-Hernandez, and E. Delgado-Alvarado, "A novel version of HPM coupled with the PSEM method for solving the blasius problem," *Discrete Dynamics in Nature and Society*, vol. 2021, Article ID 5909174, 12 pages, 2021.

[42] N. Anjum, Ji-H. He, Q. T. Ain, and D. Tian, "LI-HE'S modified homotopy perturbation method for doubly-clamped electrically actuated microbeams-based micro-electromechanical system," *Facta Universitatis – Series: Mechanical Engineering*, vol. 19, no. 4, p. 601, 2021.

[43] Y. O. El-Dib, N. S. Elgazery, A. A. Mady, and H. A. Alyousef, "On the modeling of a parametric cubic-quintic nonconservative duffing oscillator via the modified homotopy perturbation method," *Zeitschrift für Naturforschung A*, vol. 77, no. 5, pp. 475–486, feb 2022.

[44] S. Ahmad, A. Ullah, A. Akgül, and M. De la Sen, "A novel homotopy perturbation method with applications to nonlinear fractional order KdV and burger equation with exponential-decay kernel," *Journal of Function Spaces*, vol. 2021, Article ID 8770488, 11 pages, 2021.

[45] S. J. Johnston, H. Jafari, S. P. Moshokoa, V. M. Ariyan, and D. Baleanu, "Laplace homotopy perturbation method for burgers equation with space- and time-fractional order," *Open Physics*, vol. 14, no. 1, pp. 247–252, jan 2016.

[46] C. Li, D. Qian, and Y. Q. Chen, "On riemann-liouville and caputo derivatives," *Discrete Dynamics in Nature and Society*, vol. 2011, Article ID 562494, 2011.

[47] X. -B. Yin, S. Kumar, and D. Kumar, "A modified homotopy analysis method for solution of fractional wave equations," *Advances in Mechanical Engineering*, vol. 7, no. 12, Article ID 168781401562033, 2015.

[48] M. A. Hegagi, "An efficient approximate-analytical method to solve time-fractional KdV and KdVB equations," *Information Sciences Letters*, vol. 9, no. 3, pp. 189–198, 2020.